UNIVERSITI
TEKNOLOGI
PETRONAS

DISSERTATION REPORT FYP

STUDY ON THE MANUEVERABILITY OF AN UNDERWATER GLIDER WITH APPENDAGES

By

GEENEISH SIVALINGAM

14788

Supervisor

DR MARK OVINIS

JAN 2014

Universiti Teknologi PETRONAS

Bandar Seri Isandar

31750 Tronoh,

Perak Darul Ridzuan

ABSTRACT

This paper presents the hydrodynamic analysis with the aim of determining the underwater glider with appendage maneuverability performance. The external appendage would affect the behaviour of the underwater glider. Computer Aided Design (CAD) is used to deal with the geometric variation of the underwater glider. Based on the design model, a simulation system using Computational Fluid Dynamics (CFD) for the underwater glider is established. The different velocities are simulated to analyse the hydrodynamics of the underwater glider. In order to evaluate the influences of appendage on the maneuverability performance of the underwater glider, simulations of underwater glider with and without appendage are performed and compared. The results demonstrate that the underwater glider with appendage shows higher drag force, high pressure coefficient and high velocity zone where the ability to maintain its gliding path is unsymmetrical, resulting in poor turning performance.

Table of Contents

LIST OF FIGURES

LIST OF TABLE

LIST OF EQUATION

1 INTRODUCTION

1.1 Background Study

Underwater gliders are a class of autonomous underwater vehicles (AUVs). They glide through the ocean using their wins and tails, controlling their buoyancy using ballast system and their attitude by moving their internal masses. AUVs is being utilised in many applications, e.g. oceanographic research, offshore-mineral exploration, fisheries-acoustics, deep-sea exploration and coastal defence by Fernandes [1].They are preferred for their low cost, autonomy and capability for long range, extended-duration deployments. Most underwater gliders being used in the underwater industry are without appendages. Asha Bender et al. [2] states that the drawbacks of this AUVs are having a small set of sensors available to describe their environment and have limited power and memory sources. Therefore to explore the application of AUV, which existed, the AUV may carry equipment with the external appendage. Many scholars have conducted research on modelling and simulation of AUV as noted in Song et al. [3] and Evans and Nahon [4]. Zhang et al. [5] used CFD software to calculate hydrodynamic coefficients and simulated the maneuverability of AUV utilizing the coefficients and simulation system, which have been done in support of this paper AUV design. Yumin et al. [6] experiment shows that the stability and recovering rate is better of underwater glider with appendages but the turning performance shows a poor result.

1.2 Problem Statement

The effect of external appendages on the hydrodynamics of the AUV and its maneuverability performance of the AUV which is the main concern. The hydrodynamic behaviour of underwater glider with appendages is still poorly understood.

1.3 Objectives

The objective of this project is to focus on underwater glider with appendages whereby to study the hydrodynamic forces of the underwater glider and to study the effect of the external appendages on the maneuverability performance of the underwater glider with appendage. A comparison based on the maneuverability performance of underwater glider with and without appendage is done.

1.4 Scope of Study

The scope of the study consists of creating the 3D solid model and determining the hydrodynamic forces of underwater glider with appendages and maneuverability performance through simulation. Equations of Motion and the forces acting on the underwater glider with appendages are derived. CAD module (computer-aided design) is used to model and design the underwater glider with appendages while CFD module (Computational Fluid Dynamics) is used to study the hydrodynamics of the underwater glider with appendages and to perform analysis on the maneuverability performance of the AUV. The result is then compared with Alvarez [7] to validate the simulation.

2 LITERATURE REVIEW

Underwater gliders are widely use while those with external appendages are uncommon. The three mainly used underwater glider designs are Slocum, Spray and Sea glider. Joshua [8] states that these designs have several features of interest towards the configuration and motion of underwater glider, including:

- A design without a buoyancy system, propelled by a drop weight
- Ballast systems to control buoyancy.
- Moving internal masses to control attitude, using one or two masses.
- Symmetrical designs with fixed wings for gliding both up and down.
- External surfaces for control, including a rudder.
- Wings of varying size, location and geometry.
- Tail surfaces that change angle at inflection from downwards to upwards glide

Underwater glider with appendages is an innovation of the current design in the world. This external appendage will increase the function on underwater glider since space will not be a factor. There are still studies going on regarding how the external appendage affects the hydrodynamic design of the underwater glider.

According Yumin et al. [6]

> Experiment data shows the stability criterion of the AUV with appendage is higher compared to without appendage. Simulation of vertical trapezoid maneuver shows that the executing time and over depth of the AUV with appendage is faster and shorter due to higher metacentric height.

The pitch angle of AUV without appendage is smaller than AUV without appendage. Hence, the surge velocity of AUV with appendage is slower compared to AUV without appendage in Graver [8]. Brender [2] found that the turning performance of AUV with appendage is poor. The reason is that this AUV is unsymmetrical on a horizontal plane and the vertical force is also different.

3 METHODOLOGY

3.1 Research Methodology

To examined the AUV's performance in the simulation manner; hydrodynamic equations of motion should be established, then hydrodynamic forces and moment's values should be fed to the equations of motions, and simulation studies should be performed in required maneuvering scenarios. In this study, 3D solid modelling program CATIA, ANYSYS GAMBIT and TGRID meshing programs and ANYSYS FLUENT commercial program is used as shown in Figure 1.

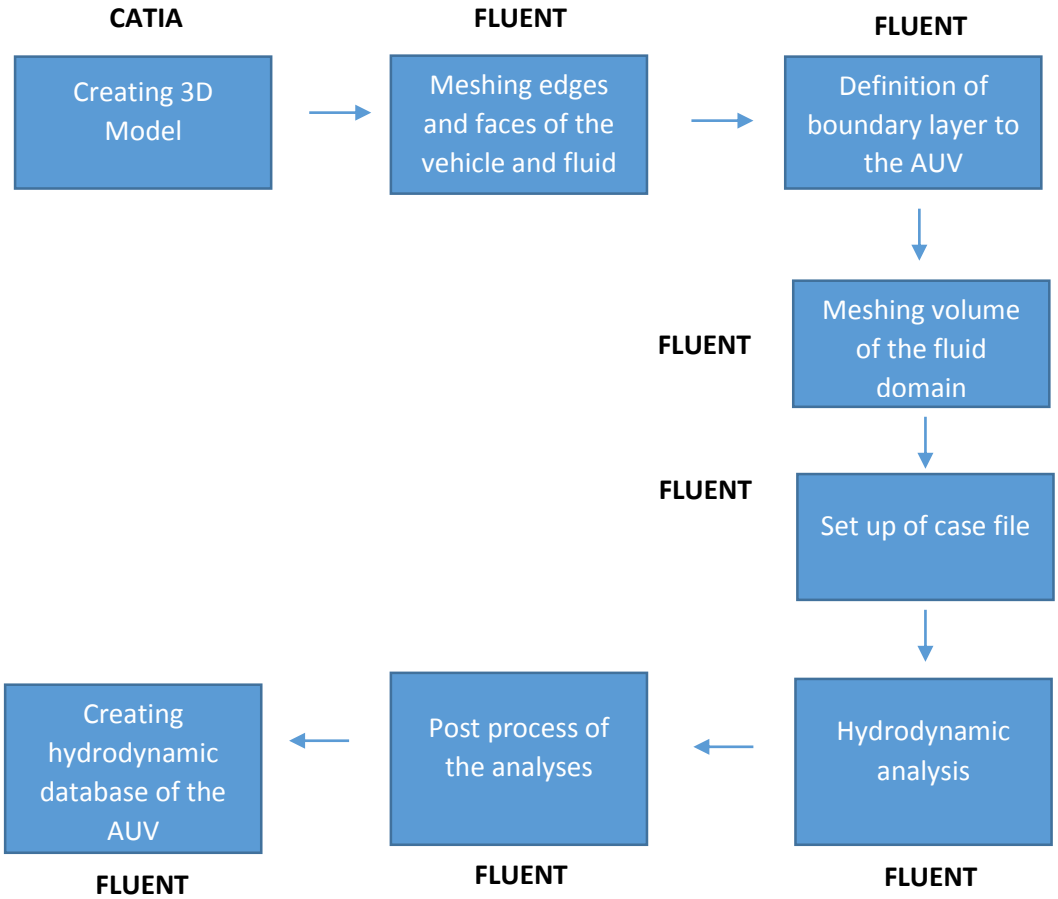

Figure 1: Methodology of the Simulation

3.2 Key Milestone

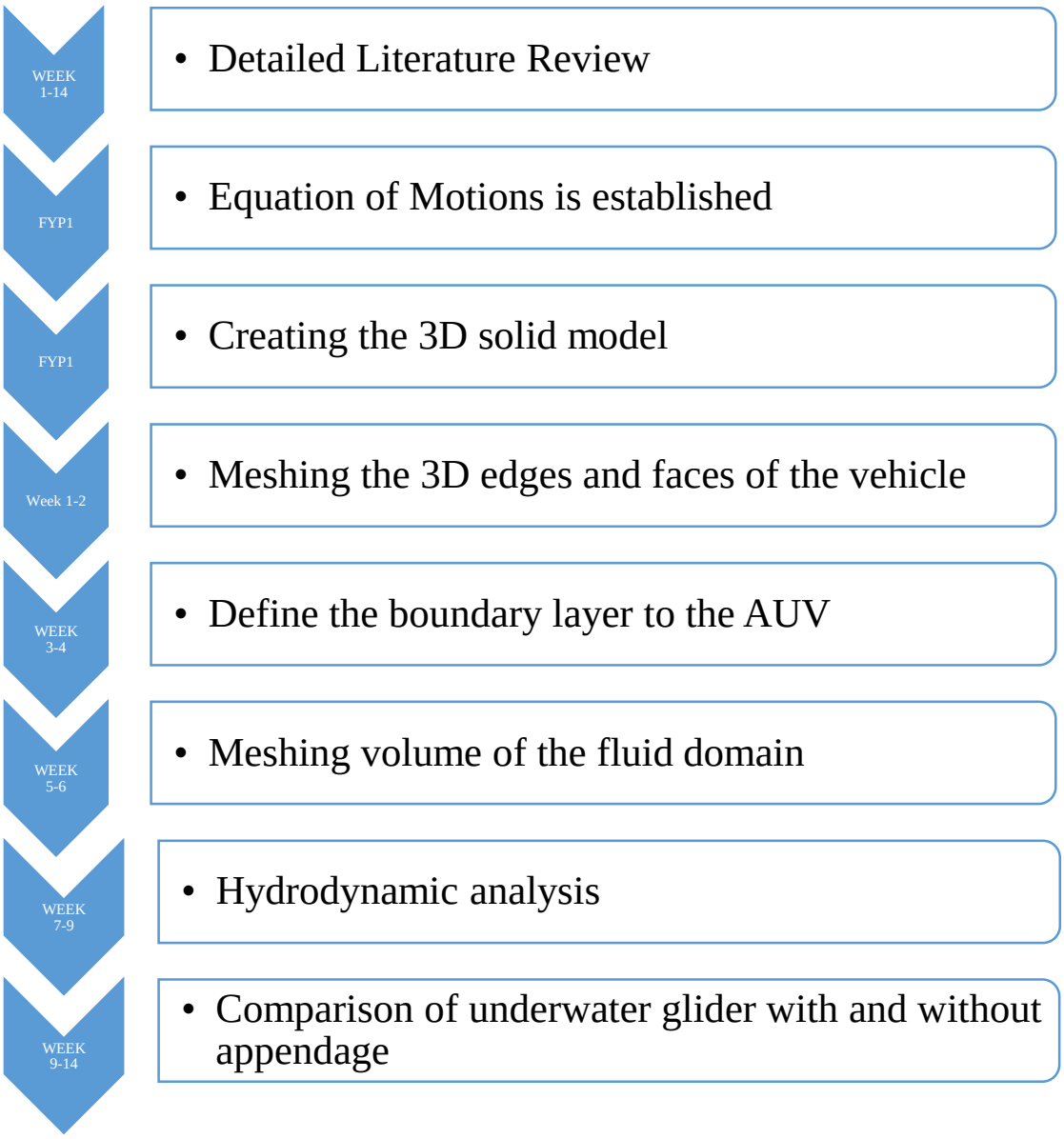

3.3 Gantt chart

NO	Detail	Weeks														
		FYP1	1	2	3	4	5	6	7	8	9	10	11	12	13	14
1	Detailed Literature Review															
2	Equation of Motions															
3	Creating 3D solid model															
4	Meshing 3D edges and faces of the vehicle															
5	Define the boundary to the AUV															
6	Meshing volume of the fluid domain															
7	Hydrodynamic analyses															

4 RESULTS AND DISCUSSION

4.1 Definition of the Hydrodynamic Coefficients

The coefficients which mostly affect the maneuverability of the AUV are static and the linear damping coefficients. A rectangular Cartesian coordinate system attached to the vehicle as shown in Figure 2.

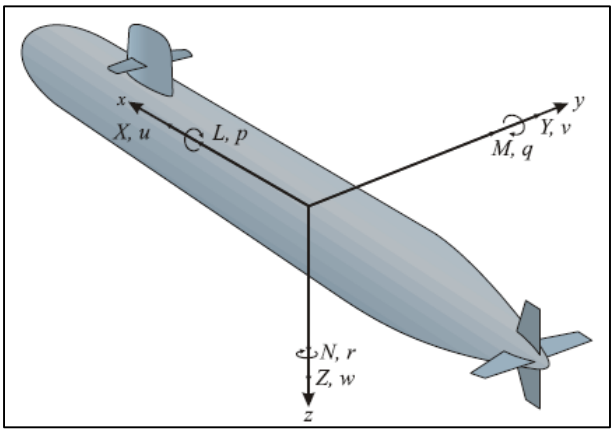

Figure 2: Cartesian coordinate system of the AUV

The three components of the hydrodynamic force along the directions x, y, z are denoted by X, Y, Z respectively and three components of the hydrodynamic moments by L, M, N. The three components of force X, Y, Z and the three components of moments L, M, N are expanded up to second order terms in the linear and angular velocities u, v, w, p ,q, r and the coupled of them.

4.2 CAD Module

We consider axis-symmetric bodies with the circular cross section and the geometry is parameterized by three length parameters (i.e. length of nose (L_n), length of parallel middle body (L_m), length of the tail (L_t)), one cross sectional parameter (i.e. nose coefficient-n_n and tail coefficient$-n_t$. According to Alvarez et al. [9] the tail and nose radii are defined :

$$r_t = \frac{D_{max}}{2}\left(1 - \left(\frac{x - L_n - L_m}{L_t}\right)^{n_t}\right);\ r_n = \frac{D_{max}}{2} = \left(1 - \left(\frac{L_n - x}{L_n}\right)^{n_n}\right)^{\frac{1}{n_n}} \qquad \textbf{Equation 1}$$

Where r_t and r_n are the radius of tail and nose respectively, x is the position along L and all other parameters are mentioned above.

The parameterization of hull geometry is shown in Figure 3:

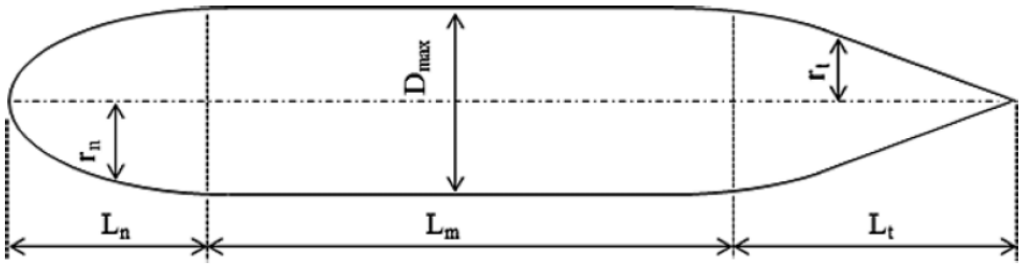

Figure 3: Parameterization of the hull geometry of the AUV

Table 1 gives the value of the parametrization of the hull geometry:

Table 1: Value of the parameterization of the hull geometry of the AUV

Vehicle particulars	Geometry of the parent hull AUV
Nose Length (L_n), mm	240
Parallel middle body length(L_m), mm	800
Tail length(L_t), mm	380
Length overall (L), mm	1420
Nose variation parameter (n_n)	2.3
Tail variation coefficient(n_t)	3
Length to diameter ratio $\left(\frac{L}{D_{max}}\right)$	8.875

The length and diameter of the parent hull body are 1.42m and 0.16m respectively. The geometry of the parent hull AUV was generated in CATIA v5 as shown in Figure 4.

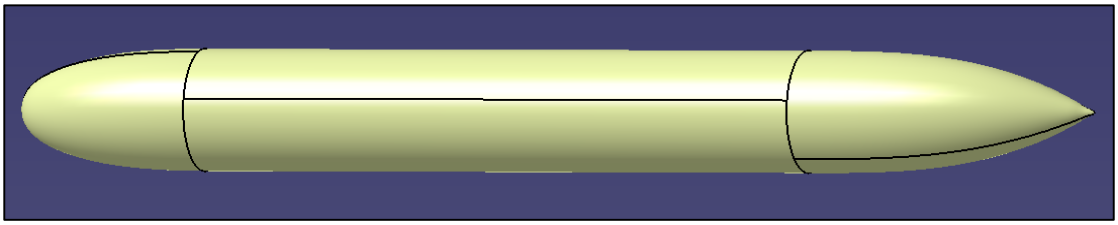

Figure 4: Parent hull AUV

The appendage is similar to the body shape and its length and diameter are 0.72m and 0.08m respectively. The geometry of the underwater glider with appendages was generated in CATIAv5 as shown in Figure 5.

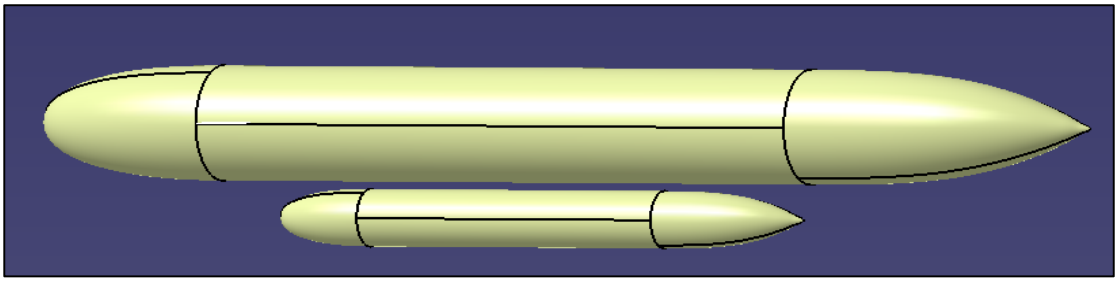

Figure 5: AUV with appendage

4.3 CFD Module

We use CFD software (i.e. ANSYS 15.0) for the estimation of viscous drag and velocity distribution of the body. The Shear Stress Transport (SST) k-ω model is a two equation eddy-viscosity model developed by Menter [9] that blends the k-ω model in the near wall region with the free stream independence of the k-ε model in the far field making it robust, accurate and most effective.

According to Alvarez et al. [7]

The SST k-ω model includes the following refinements to the k-ω model:

- The standard k-ω model and transformed k-ε model are both multiplied by a blending function and added together
- The blending function is assigned such that it will be one in the near-wall region, which activates the transformed
- The SST model has a damped cross function derivative term in the ω equation.

These features make the SST k-ω model suitable for a wider class of flows, such as adverse pressure gradient flows, air foils, transonic and shock waves, etc., than the standard k-ω model. The use of the k-ω model in the boundary layer zone makes the model directly usable down to the wall through the viscous sub-layer.

4.4 Boundary Conditions

No slip condition was imposed over the surface of the axis-symmetric body. The upstream boundary of the domain is modelled as velocity inlet (inflow) and the downstream boundary of the domain is modelled velocity outlet (outflow). All other boundaries of the 3-D rectangular domain experienced the slip condition. The boundary conditions, along with fluid domain definitions, are shown in Figure 6.

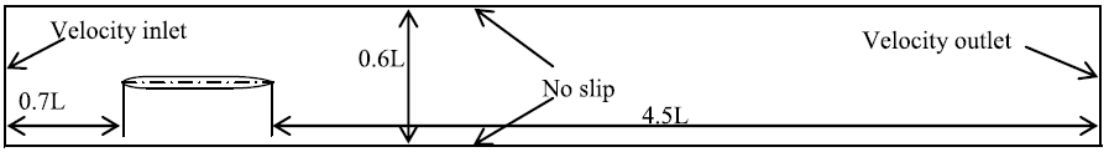

Figure 6: Fluid domain with boundary conditions in CFD

4.5 Mesh Generation

We use a structured mesh, with the mesh finer near the body and coarser away from the body where the method used in assembly meshing is tetrahedrons. The finer mesh on the glider body is shown in Figure 7 while the mesh of the whole underwater glider in the fluid domain is shown in Figure 8. After meshing, the CFD computations are done iteratively to estimate the drag.

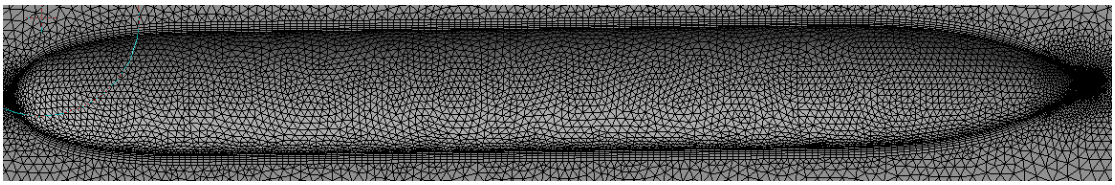

Figure 7: Mesh generated on the body

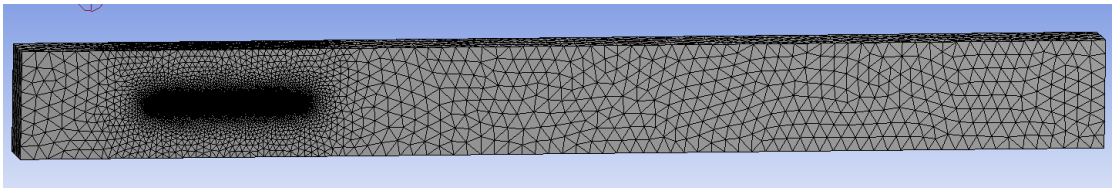

Figure 8: Mesh of the fluid domain

4.6 Experimental Validation

The experimental validation of the results is performed by considering the experimental data available in the literature for the investigated basic model of AUV, Alvarez et al. (2009) [9]. Table 2 shows the comparison of drag coefficient obtained from experiment (Alvarez et al.) where the percentage error increases as the velocity increases.

Table 2: Comparison of drag coefficient obtained from experiment and CFD

Velocity, (m/s)	Drag Coefficient		Percentage error, (%)
	CFD	Alvarez et al. 2009	
0.5	0.005686	0.00570	0.25
1.0	0.005014	0.00517	3.02
1.5	0.004684	0.00489	4.21
2.0	0.004470	0.00472	5.39

Figure 6 shows the validation of the basic AUV model for different velocities. Results indicate that the CFD model underestimates the drag coefficient. Surprisingly, the differences found between the measured and computed values are not too big considering the rough models employed to estimate friction and form of resistance coefficients.

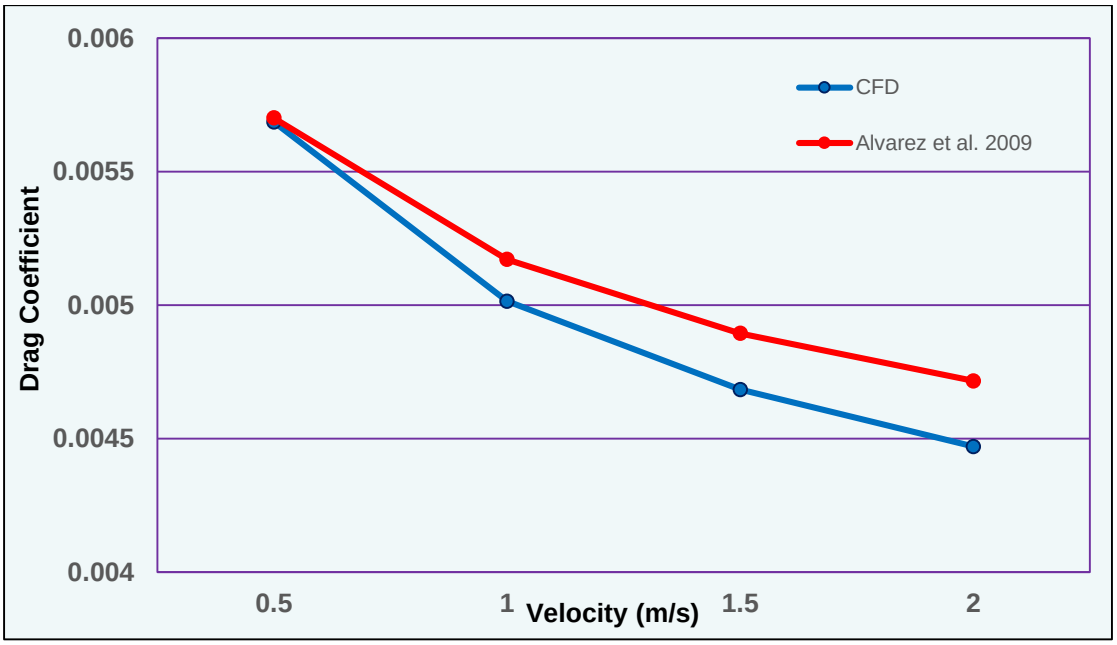

Figure 9: Drag Coefficient obtained from experimental and CFD

4.7 Hydrodynamic analysis

In the two designs (i.e. underwater glider with appendages and without), the wetted surface areas for the two designs are different, $0.652m^2$ and $0.996m^2$ respectively. Hence this effects the drag force obtained. Table 3 shows the computed drag result for underwater glider with and without appendage.

Table 3: The computed drag result of underwater glider with and without appendage

Velocity, (m/s)	Parent hull			Parent hull with appendages			Increase in drag, %
	Viscous pressure coefficient, (C_{pv})	Skin friction coefficient, (C_f)	Drag, (N)	Viscous pressure coefficient, (C_{pv})	Skin friction coefficient, (C_f)	Drag, (N)	
0.5	10.46 x 10^{-4}	46.41 x 10^{-4}	0.463	64.43 x 10^{-5}	40.57 x 10^{-4}	0.584	26.13
1.0	88.39 x 10^{-5}	41.31 x 10^{-4}	1.632	58.06 x 10^{-5}	33.84 x 10^{-4}	1.971	20.77
1.5	81.47 x 10^{-5}	38.69 x 10^{-4}	3.429	55.62 x 10^{-5}	30.45 x 10^{-4}	4.028	17.47
2.0	77.47 x 10^{-5}	36.95 x 10^{-4}	5.818	54.24 x 10^{-5}	28.30 x 10^{-4}	6.706	15.26

The skin friction drag is caused by viscous drag in the boundary layer around the object. The boundary layer at the front of the object is usually laminar and relatively thin, but becomes turbulent and thicker towards the rear. The position of transition depends on the shape of the object.

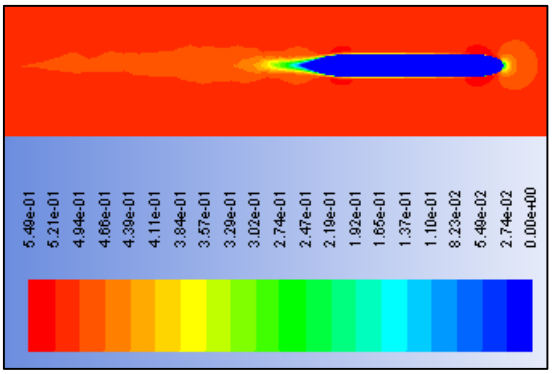

Figure 10 a: Velocity contours around surface of underwater glider (v=0.5m/s)

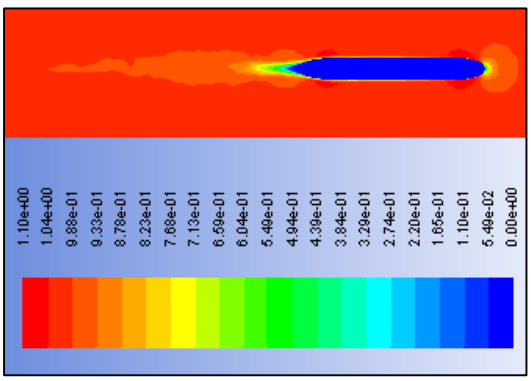

Figure 10 i: Velocity contours around surface of underwater glider (v=1.0m/s)

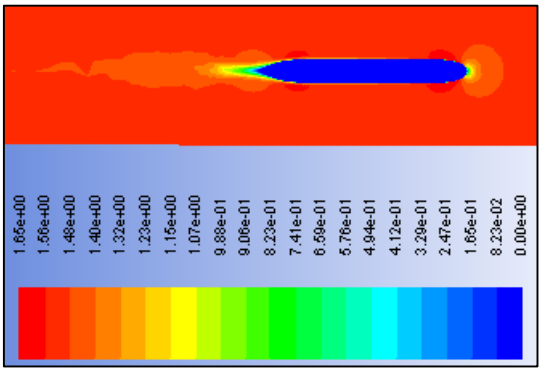

Figure 10 c: Velocity contours around surface of underwater glider (v=1.5m/s)

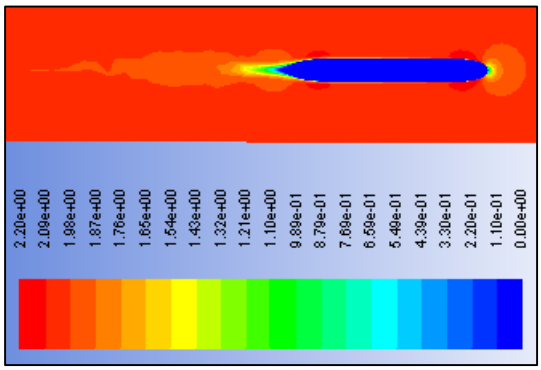

Figure 10 d: Velocity contours around surface of underwater glider (v=2.0m/s)

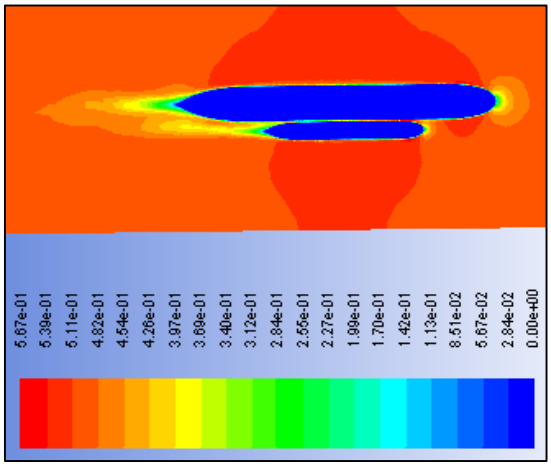

Figure 11 a: Velocity contours around surface of underwater glider with appendage (v=0.5m/s)

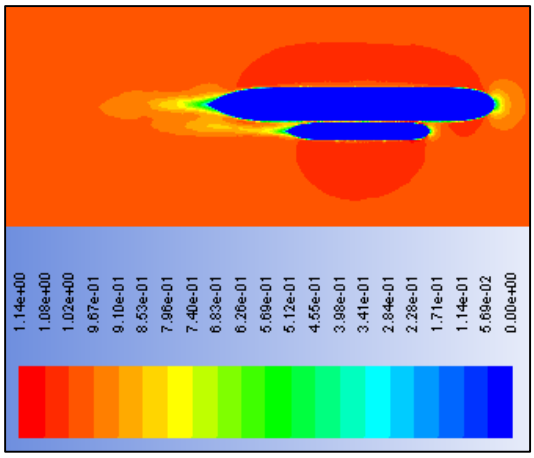

Figure 11 b: Velocity contours around surface of underwater glider with appendage (v=1.0m/s)

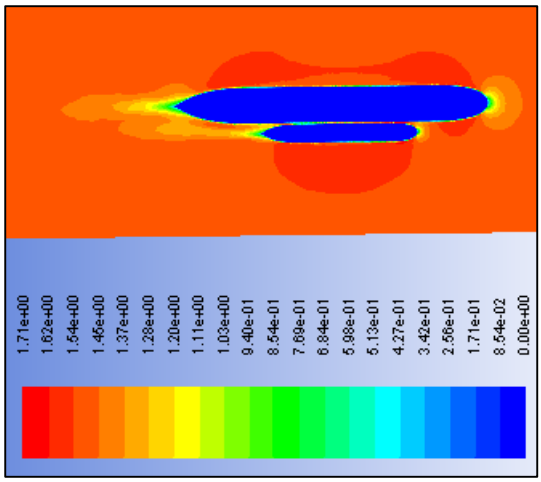

Figure 11 c: Velocity contours around surface of underwater glider with appendage (v=1.5m/s)

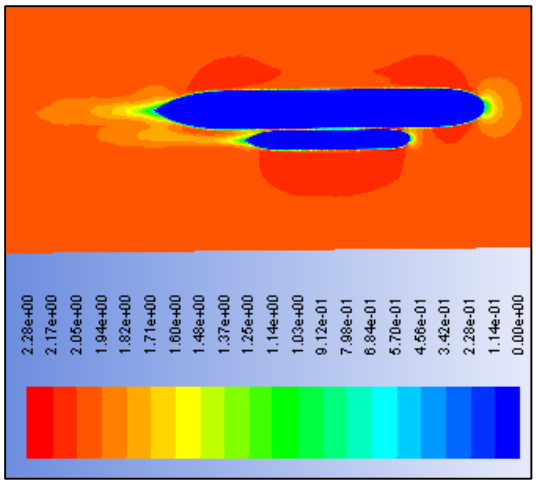

Figure 11 d: Velocity contours around surface of underwater glider with appendage (v=2.0m/s)

Table 3 shows at higher velocities the improvement in drag is even higher e.g. at velocities 0.5m/s, 1.0m/s. 1.5m/s and 2.0 m/s the reduction in the values of the drag are 26.13%, 20.17%, 17.47% and 15.26% respectively . The velocity contour show that over the underwater glider without appendage, the zone of low velocity extends over a larger length of the body. We can observe from the velocity contours that for the underwater glider with appendage is happening close to the parallel middle region of the body and this is bound to increase drag. However, in the underwater glider without appendage, flow separation is happening close to the tail end. This reduces drag. We can observe this clearly at all speeds from 0.5 m/s to 2m/s.

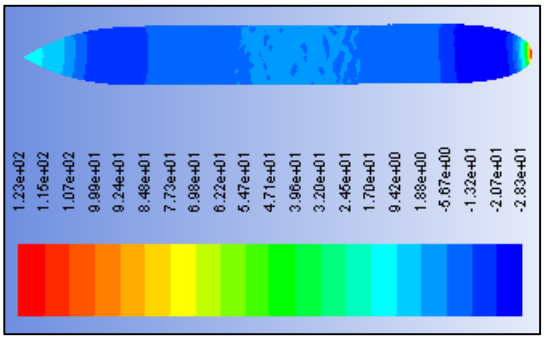

Figure 12 a: Pressure contours around surface of underwater glider (v=0.5m/s)

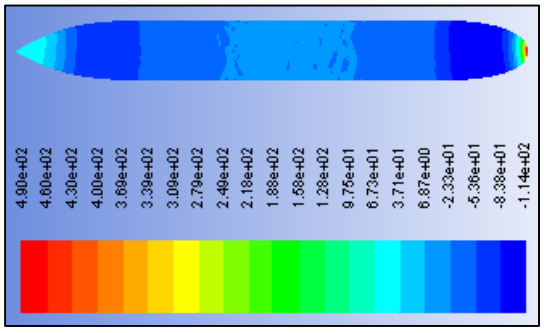

Figure 12 b: Pressure contours around surface of underwater glider (v=1.0m/s)

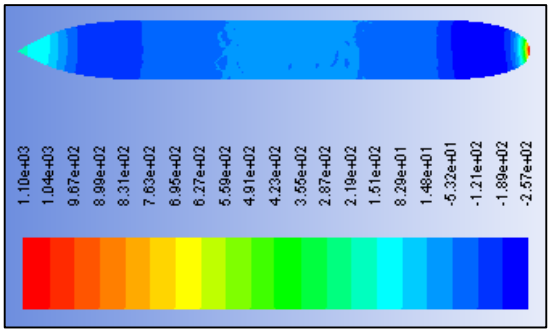

Figure 12 c: Pressure contours around surface of underwater glider (v=1.5m/s)

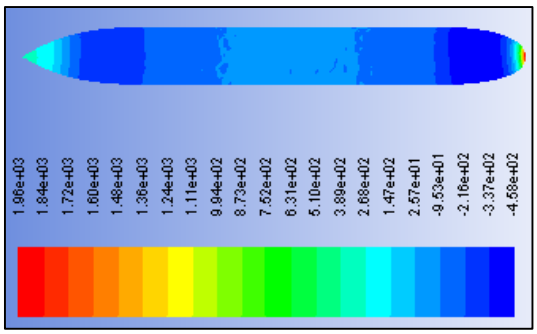

Figure 12 d: Pressure contours around surface of underwater glider (v=2.0m/s)

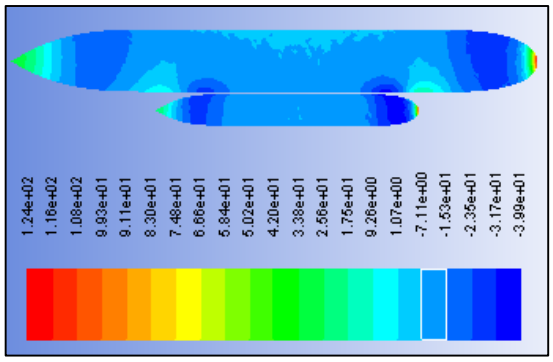

Figure 13 a: Pressure contours around surface of underwater glider with appendage (v=0.5m/s)

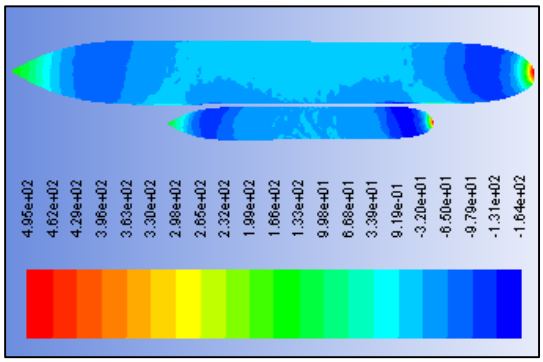

Figure 13 b: Pressure contours around surface of underwater glider with appendage (v=1.0m/s)

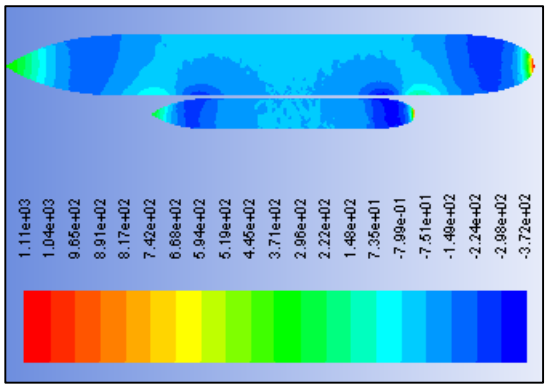

Figure 13 c: Pressure contours around surface of underwater glider with appendage (v=1.5m/s)

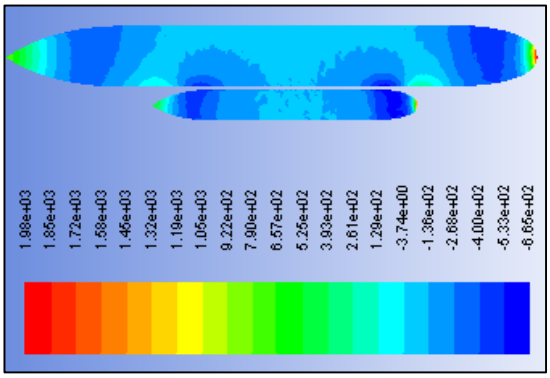

Figure 13 d: Pressure contours around surface of underwater glider with appendage (v=2.0m/s)

At v=1.0m/s, the comparison of pressure contours for underwater glider with and without appendage shows that underwater glider without appendage is covered with low values of pressure coefficient, e.g. from Figure 12 b we can clearly see that major part of the middle body of underwater glider with appendage is covered with pressure coefficient values between -0.235 to -7.11, on the other hand we can observe from Figure 13a that the large portion of the middle body of underwater glider without appendage is covered with pressure coefficient between -0.132 and 1.88. The coverage of large surface area with high pressure coefficient is expected to result in increase of drag of underwater glider without appendage. This phenomenon is the same for higher velocities also and the difference can be observed between Figure 12a and 13a, Figure 12c and 13c and Figure 12d and 13d.

5 CONCLUSION AND RECOMMENDATION

This paper has presented the maneuverability performance of the underwater glider with appendage. The hydrodynamic forces based on the drag, velocity contour and pressure contour is obtained and compared between the underwater glider with and without appendage. Results have shown that the drag force of underwater glider with appendage is higher compared to without appendage but the drag decreases as the velocity decreases. Underwater glider with appendage shows high zone of pressure distribution which indirectly increases the drag coefficient. Uneven and high velocity distribution around the underwater glider with appendage shows that the ability to maintain its gliding path is unsymmetrical resulting in poor turning performance.

However in the present work the module has been restricted to only hydrodynamic calculation such ad drag, velocity and pressure distribution. In a real design process other criteria (e.g. dynamics of vehicle, control with fins, navigational and sensing requirements and weight distribution) also influence the maneuverability performance of underwater glider. It will be interesting to investigate the surge maneuver, turning circle maneuver, horizontal and vertical trapezoid maneuver.

6 REFERENCES

[1] F. P.G, Autonomous Underwater Vehiclefuture platforms for fisheries acousitics, 2003.

[2] Asher Brender, Daniel Mathew, Analysis of an Autonomous Underwater Vehicle, Sydney, 2006.

[3] Song Feijun, An PE, Folleco A, "Modelling and Simulation of autonomous underwater vehicles: design and implementation," *IEEE Journal of Oceanic Engineering,* vol. 28(2), pp. 283-296, 2003.

[4] N. M. Evans J, Dynamics modeling and performance evaluation of an auntonomous underwater vehicle, Ocean Engineering, 2004.

[5] Z. he and Y. Xu, "Using CFD software to calculate hydrodynamic coefficients," *Journal of Marine and Science Application,* pp. 149-155, 2010.

[6] Yumin Su, Jinxin Zhao,Jian Chao and Guancheng Zhang, Dynamics Modelling and Simulation of Autonomous Underwater Vehicle, Harbin University Engineering, 2012.

[7] Alvarez, A, Bertram V, Gualdesi, L, "Hull hydrodynamic otimization of autonomous underwater vehivles operating at snorkeling depth.," in *Ocean enginnering*, 2009, pp. 105-112.

[8] J. G. Graver, Underwater Gliders: Dynamics, Control and design, Princeton University, 2005.

[9] Z. Jinxin, The hydrodynamic performance calculation and motion simulation of an AUV with Appendages, Harbin Engineering University, 2011.